A finite-volume solution to the geophysical electromagnetic forward problem using unstructured grids

Hormoz Jahandari and Colin G. Farquharson

Memorial University
Department of Earth Sciences
St. John's, Newfoundland, Canada

SEG annual meeting, Houston
September 23, 2013

Contents

- Model irregular structures

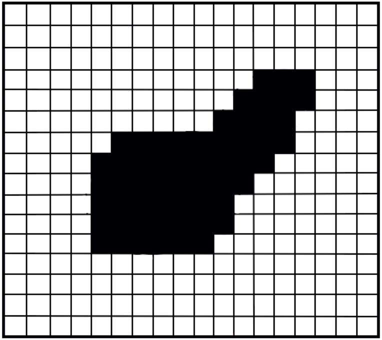

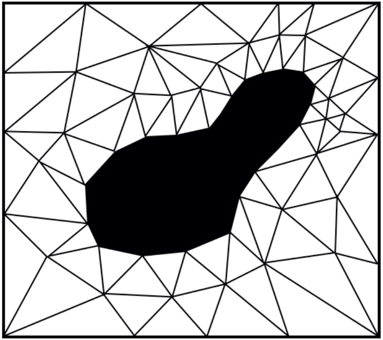

Unstructured grids

- Topographical features
- Geological interfaces

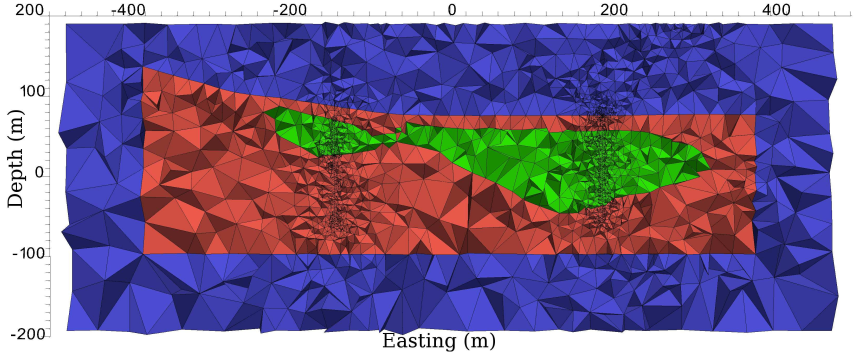

Unstructured grids

- Local refinement (at observation points, sources, interfaces)

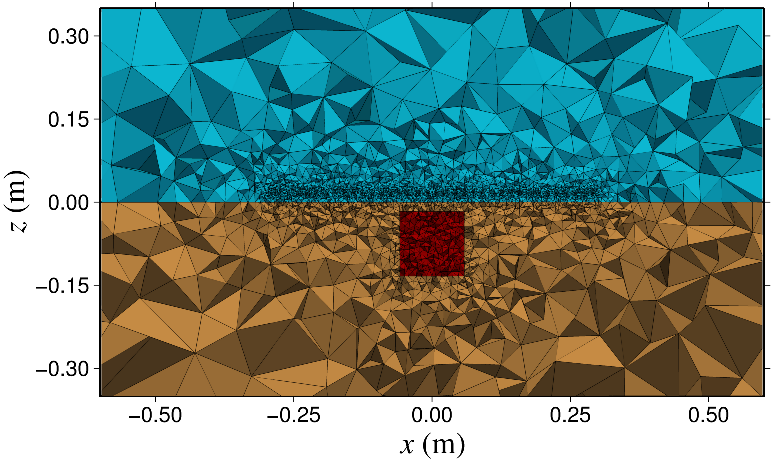

- **Grid generator: TetGen (Si, 2004)**

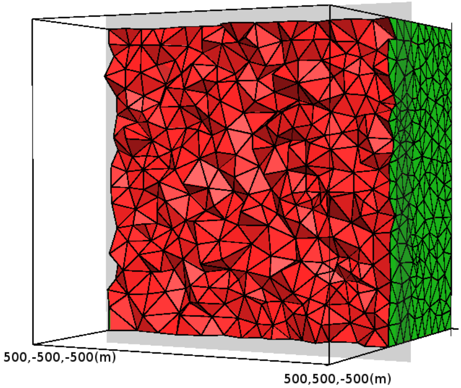

tetrahedral grid

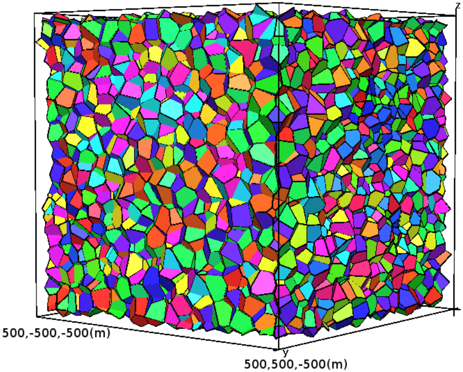

Voronoï grid

Staggered finite-volume schemes

- Magnetic field divergence free
- Easy for implementing boundary conditions
- Satisfies the continuity of tangential E
- Physically meaningful

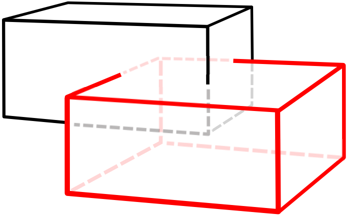

Rectilinear dual grid

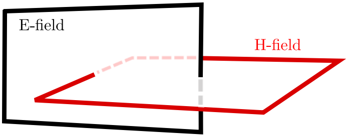

Rectilinear dual contours

Staggered finite-volume schemes

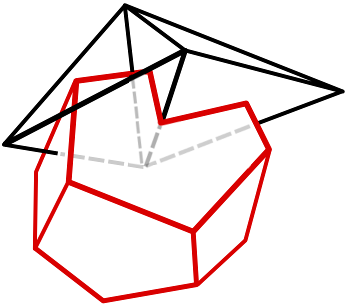

Dual tetrahedral-Voronoï grid

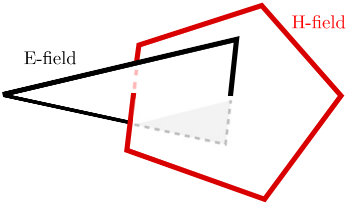

Delaunay-Voronoï contours

- **Maxwell's equations:**

$$\nabla \times \mathbf{E} = -i\omega\mu_0\mathbf{H} - i\omega\mu_0\mathbf{M}_p$$
$$\nabla \times \mathbf{H} = \sigma\,\mathbf{E} + \mathbf{J}_p$$

Helmholtz equation for electric field

$$\nabla \times \nabla \times \mathbf{E} + i\omega\mu_0\sigma\mathbf{E} = -i\omega\mu_0\mathbf{J}_p - i\omega\mu_0(\nabla \times \mathbf{M}_p)$$

- **Homogeneous Dirichlet boundary condition:**

$$\mathbf{E} = 0 \qquad \mathit{at}\ \infty$$

or

$$\mathbf{E} \cdot \tau = 0 \qquad \mathit{on}\ \Gamma$$

Finite-volume method

General features of the finite volume method

- Naturally supports unstructured grids
- Simple in idea
- Uses the integral form of equations
- Uses the average values of quantities

- **Integral form of Maxwell's equations:**

$$\oint_{\partial A^D} \mathbf{E} \cdot d\mathbf{l}^D = -i\mu_0\omega \iint_{A^D} \mathbf{H} \cdot d\mathbf{A}^D - i\mu_0\omega \iint_{A^D} \mathbf{M}_p \cdot d\mathbf{A}^D$$
$$\oint_{\partial A^V} \mathbf{H} \cdot d\mathbf{l}^V = \sigma \iint_{A^V} \mathbf{E} \cdot d\mathbf{A}^V + \iint_{A^V} \mathbf{J}_p \cdot d\mathbf{A}^V$$

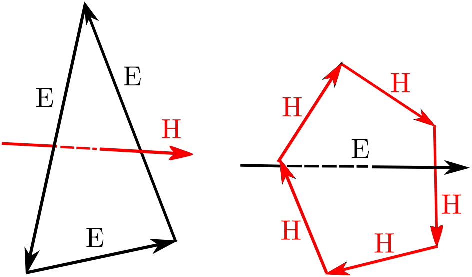

Finite-volume discretization

- **Discretized form of Maxwell's equations:**

$$\sum_{q=1}^{W_j^D} E_{i(j,q)}\, l^D_{i(j,q)} = -i\mu_0\omega H_j\, A_j^D - i\mu_0\omega M_{p_j}\, A_j^D$$

$$\sum_{k=1}^{W_i^V} H_{j(i,k)} l^V_{j(i,k)} = \sigma E_i\, A_i^V + J_{p_i}\, A_i^V .$$

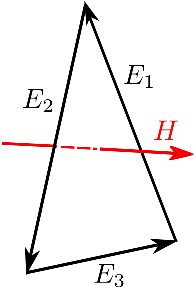

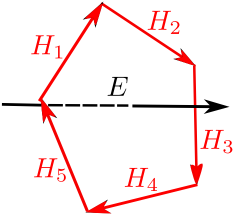

- **Discretized form of Helmholtz equation:**

$$\sum_{k=1}^{W_i^V} \left(\left(\sum_{q=1}^{W_j^D} E_{i(j,q)}\, l^D_{i(j,q)} \right) \frac{l^V_{j(i,k)}}{A^D_{j(i,k)}} \right) + i\omega\mu_0\sigma E_i\, A_i^V$$

$$= -i\omega\mu_0 \sum_{k=1}^{W_i^V} M_{p_{j(i,k)}} \frac{l^V_{j(i,k)}}{A^D_{j(i,k)}} - i\omega\mu_0 J_{p_i}$$

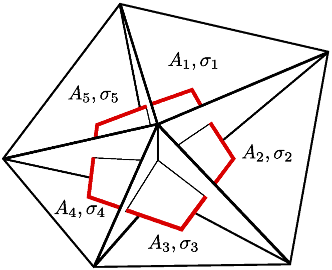

Finite-volume discretization

- **Decompose E to real and imaginary parts:**

$$E = E_{re} + iE_{im}$$

- **Resulting block matrix equation:**

$$\begin{pmatrix} \mathbf{A} & -\mathbf{B} \\ \mathbf{B} & \mathbf{A} \end{pmatrix} \begin{pmatrix} \mathbf{E}_{re} \\ \mathbf{E}_{im} \end{pmatrix} = \begin{pmatrix} \mathbf{S}_{im} \\ \mathbf{S}_{re} \end{pmatrix},$$

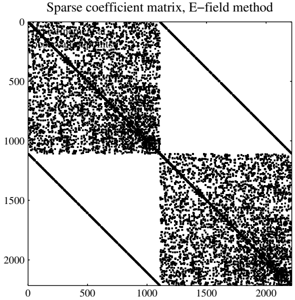

Finite-volume discretization

- **Sparse direct solver: MUMPS (Amestoy et. al, 2006)**

- **Interpolation inside tetrahedra: vector basis functions**

$$\mathbf{E}(x, y, z) = \sum_{i=1}^{6} \mathbf{N}_i(x, y, z) E_i,$$

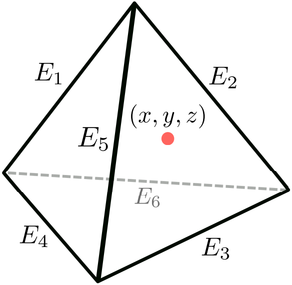

Inclusion of EM sources

- Grounded wire:

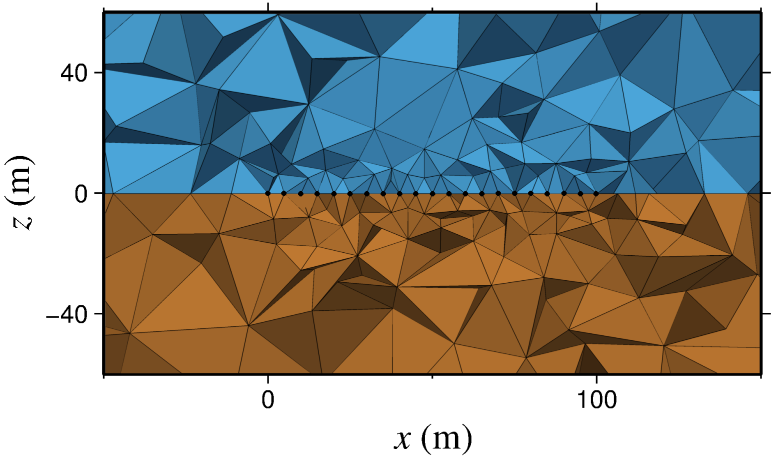

Inclusion of EM sources

- Point vertical magnetic dipole:

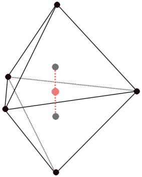

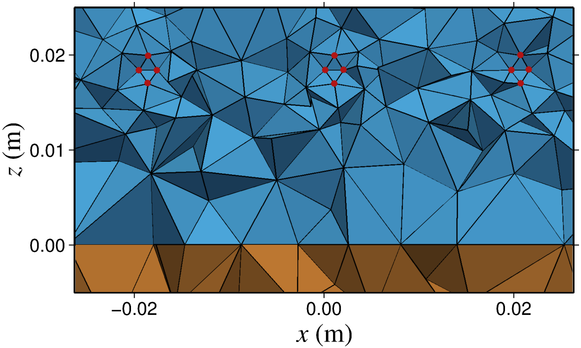

Example 1: magnetic dipole transmitter-receiver pairs

- Graphite cube in brine (physical scale modelling measurements)
- Transmitter-receiver pairs along the x axis at $z = 2\ cm$
- Dimensions of the cubic graphite: $14 \times 14 \times 14\ cm$
- $\sigma_{brine} = 7.3\ S/m$; $\sigma_{prism} = 63,000\ S/m$
- Frequencies: 1, 10, 100, 200, 400 kHz

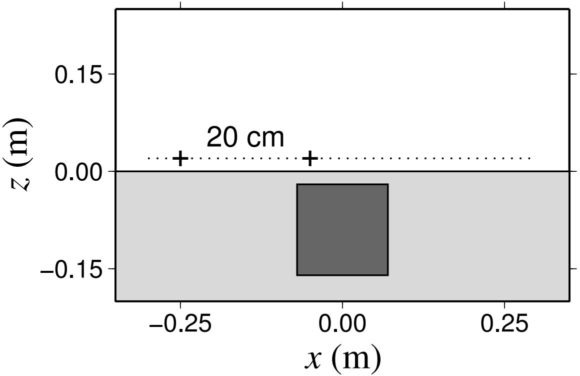

Example 1: magnetic dipole transmitter-receiver pairs

- Grid refined at the sources, observation points and the prism

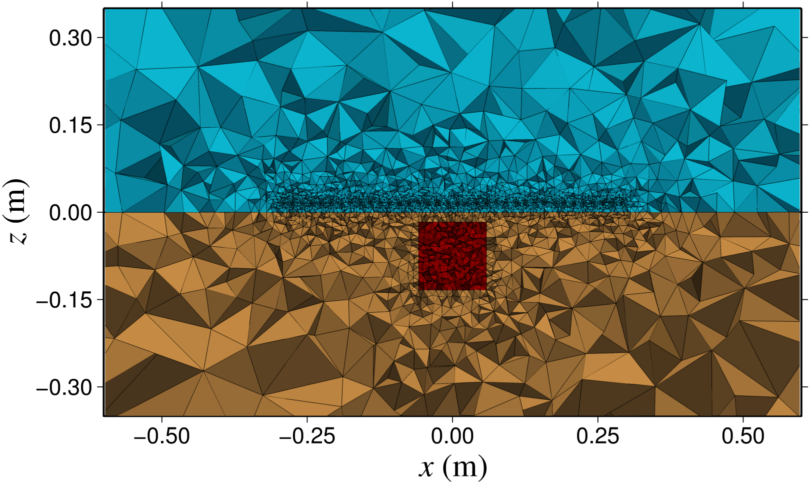

Example 1: magnetic dipole transmitter-receiver pairs

- Grid refined at the sources, observation points and the prism

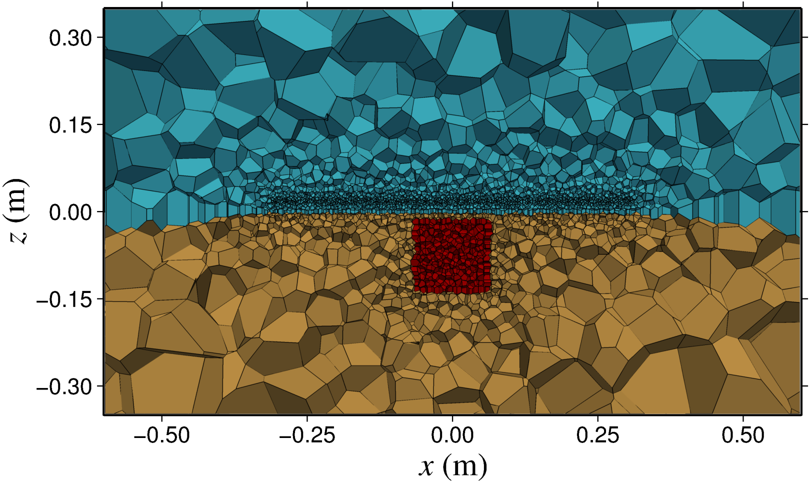

- Scattered H-field: (total−free-space)/free-space
- FV (circles) vs PSM (red), IE (orange), and FE (black)

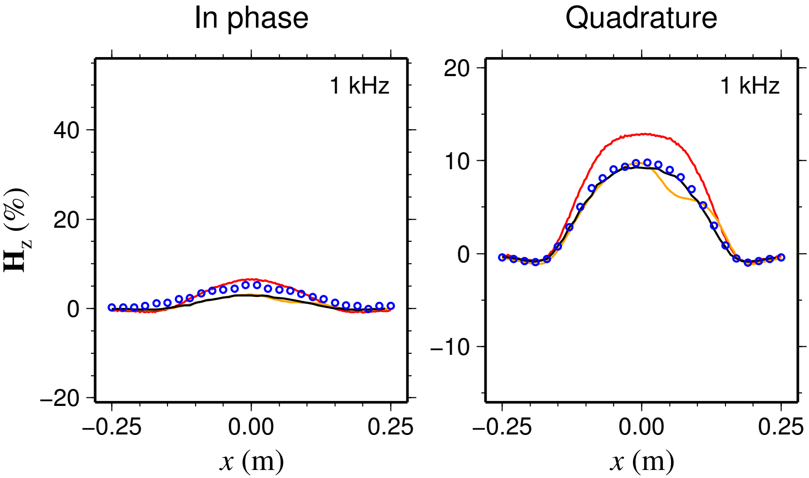

- Scattered H-field: (total−free-space)/free-space
- FV (circles) vs PSM (red), IE (orange), and FE (black)

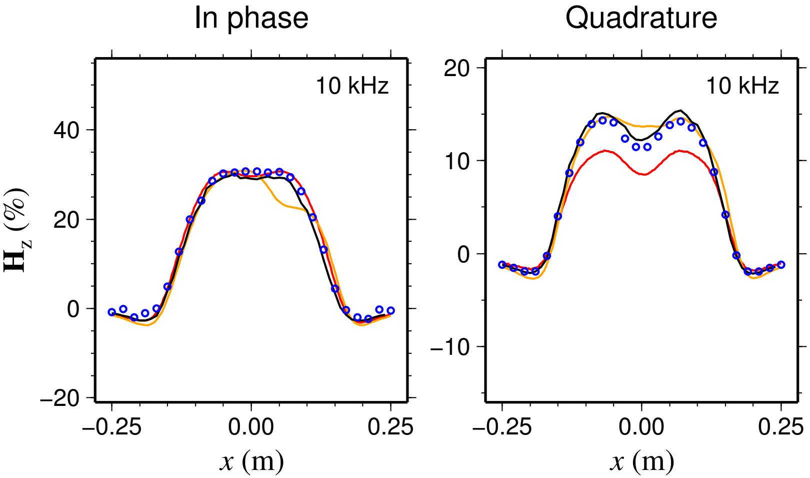

- Scattered H-field: (total−free-space)/free-space
- FV (circles) vs PSM (red), IE (orange), and FE (black)

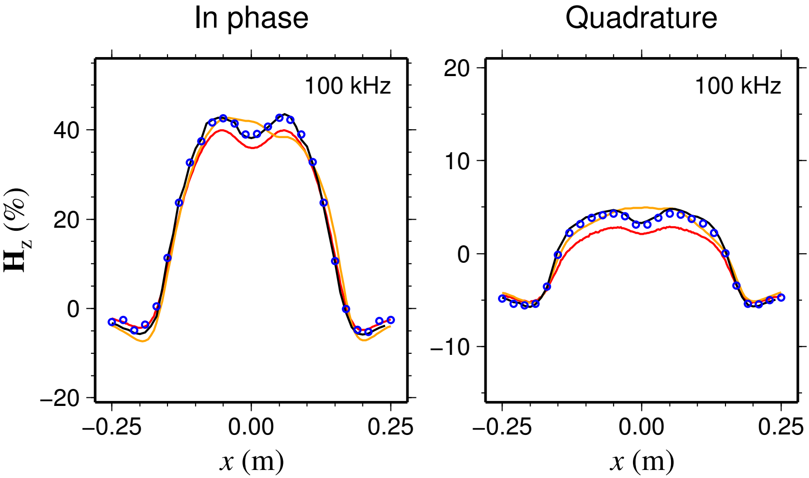

Example 1: magnetic dipole transmitter-receiver pairs

- Scattered H-field: (total−free-space)/free-space
- FV (circles) vs PSM (red), IE (orange), and FE (black)

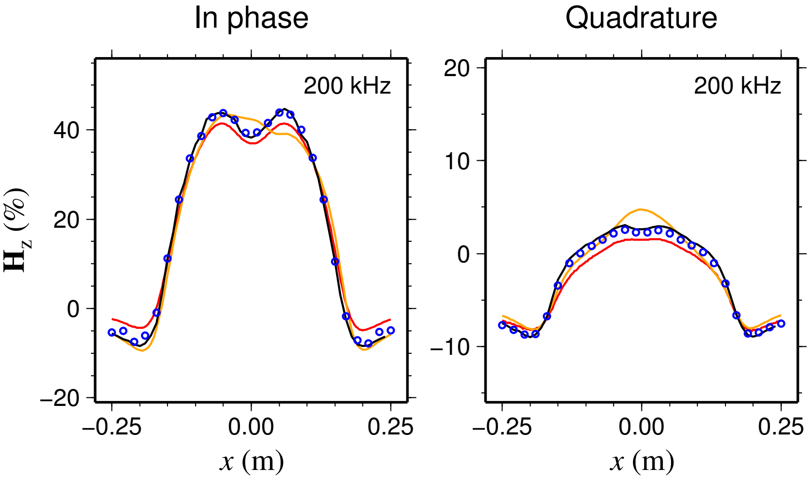

Example 1: magnetic dipole transmitter-receiver pairs

- Scattered H-field: (total−free-space)/free-space
- FV (circles) vs PSM (red), IE (orange), and FE (black)

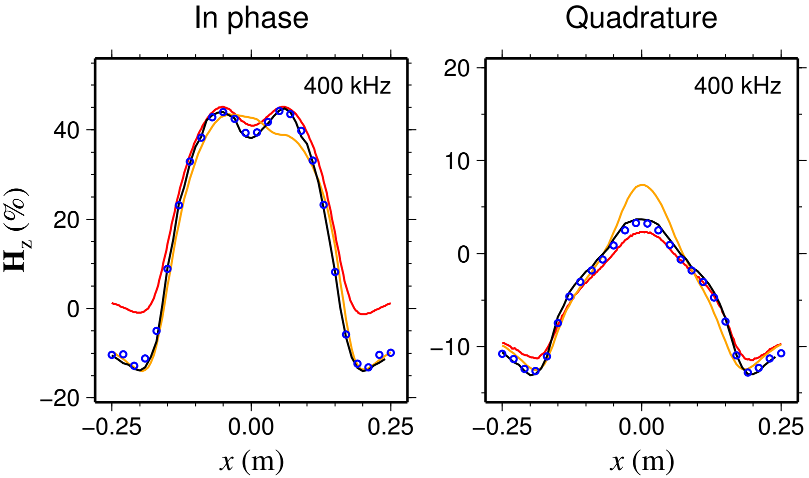

Example 1: magnetic dipole transmitter-receiver pairs

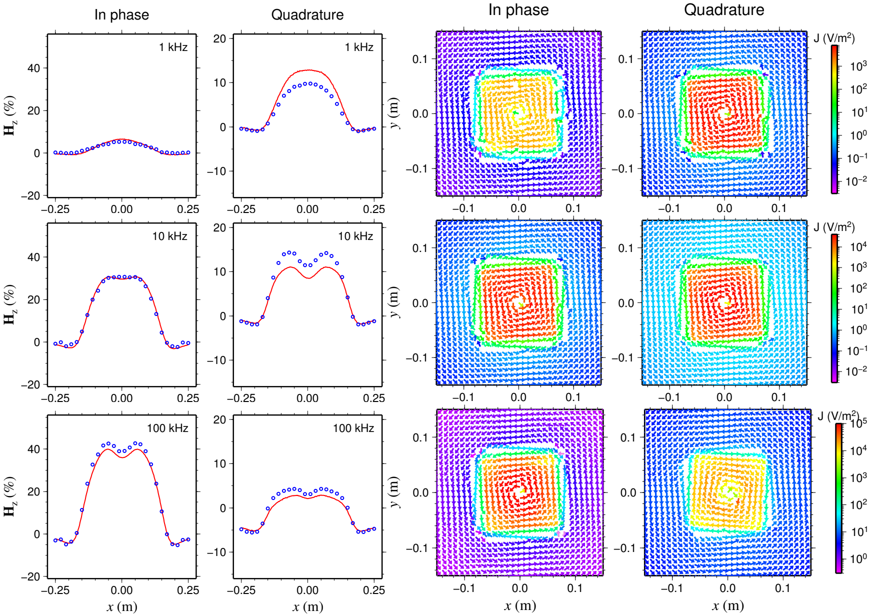

Example 2: long grounded wire

- 100 m wire along the x axis operating at 3 Hz
- Dimensions of the prism: $120 \times 200 \times 400$ m
- $\sigma_{ground} = 0.02$ S/m ; $\sigma_{prism} = 0.2$ S/m
- Observation points along the x axis

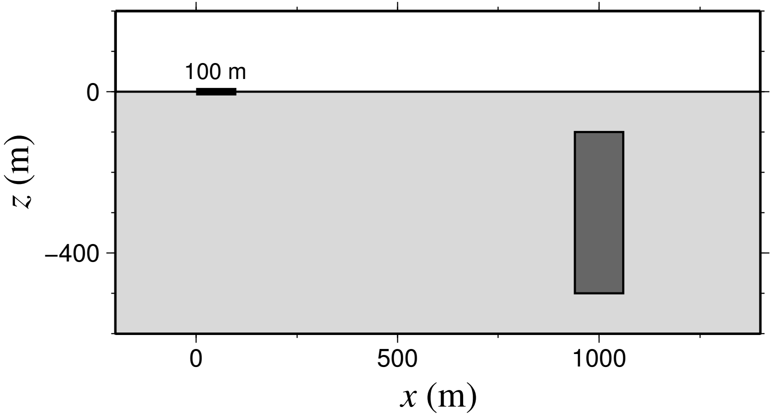

Example 2: long grounded wire

- Dimensions of the domain: $40 \times 40 \times 40$ *km*
- Number of tetrahedra: 162,689 ; number of unknowns: 189,105

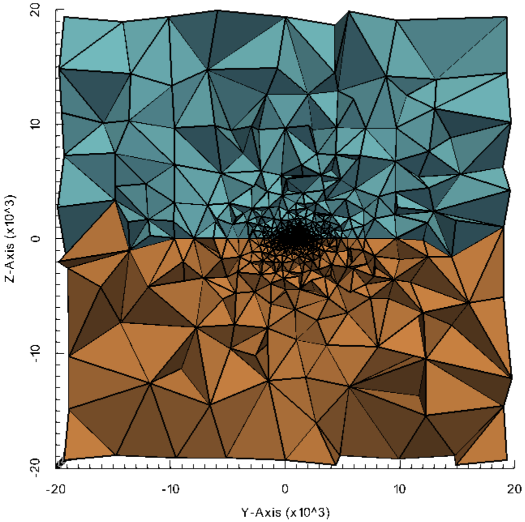

Example 2: long grounded wire

- Grid refined at the source, observation points and the prism
- Computation time: 40 *s* ; memory: 4 *Gbytes* (on Apple Mac Pro; 2.26 GHz Quad-Core Intel Xeon processor)

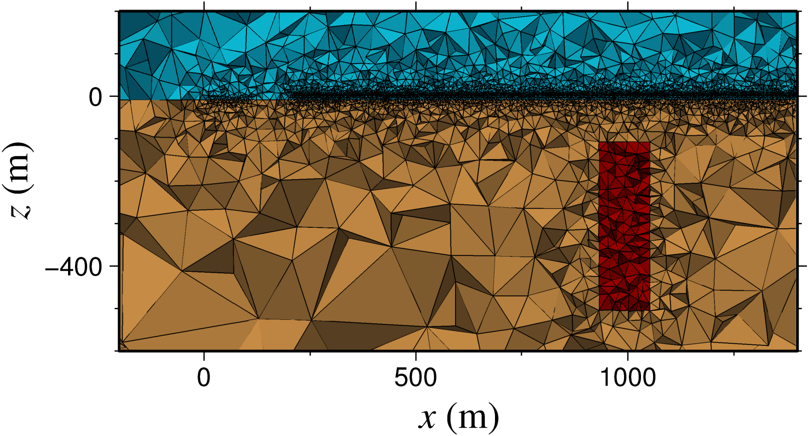

Example 2: long grounded wire

- Grid refined at the source, observation points and the prism
- Computation time: 40 *s* ; memory: 4 *Gbytes* (on Apple Mac Pro; 2.26 GHz Quad-Core Intel Xeon processor)

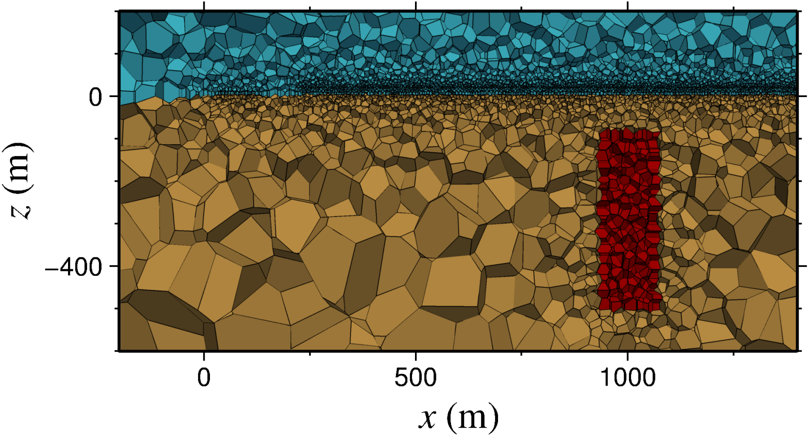

Example 2: long grounded wire

- Without prism (homogeneous halfspace)
- Total field
- FV vs IE (Farquharson and Oldenburg, 2002)

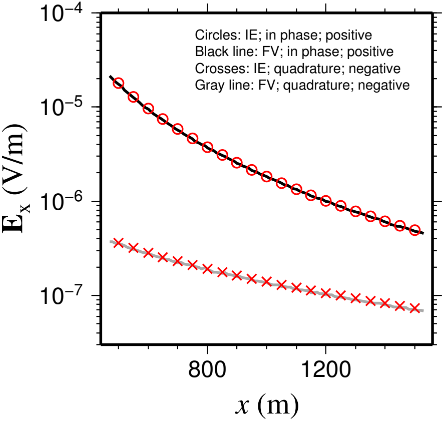

- With and without prism
- Total field
- FV only

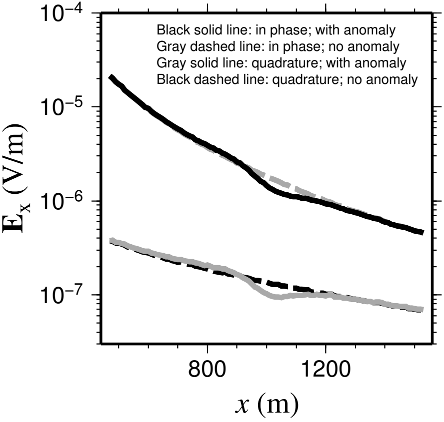

Example 1: long grounded wire

- Scattered field
- FV vs IE

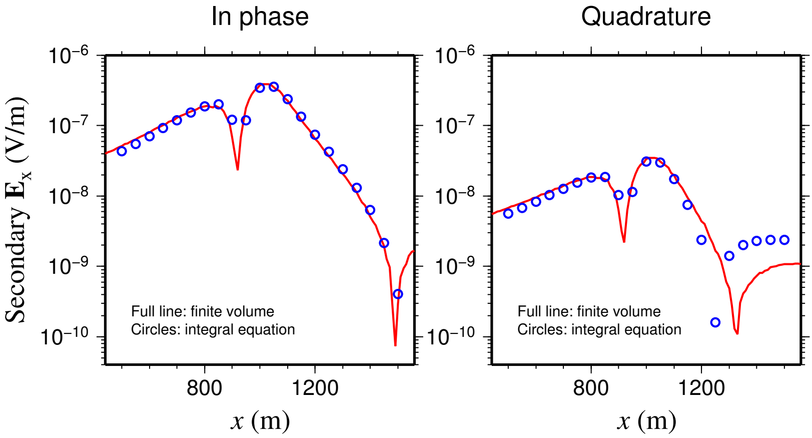

- Horizontal section ($z = -150\ m$)
- Total electric field (in phase and quadrature)

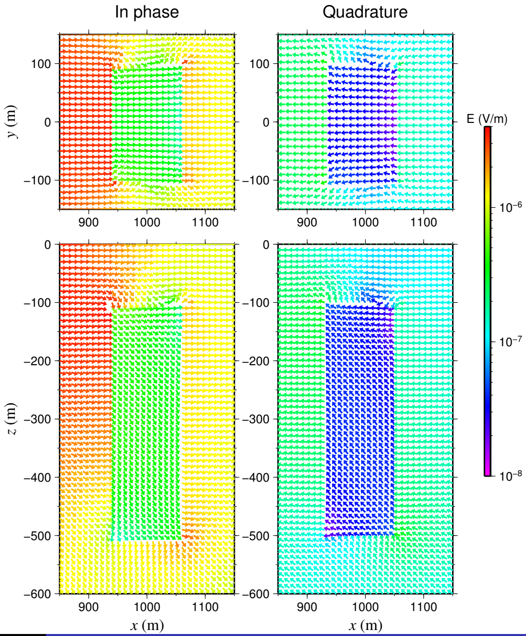

- Vertical section ($y = 0\ m$)
- Total electric field (in phase and quadrature)

Example 2: accuracy studies

- **Refinement at the observation points**
- Exact solutions: solution due to a fine grid

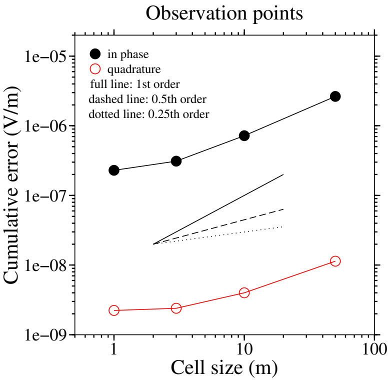

Example 2: accuracy studies

- **Improvement in grid quality**
- Qualiy criteria: maximum radius-edge ratio

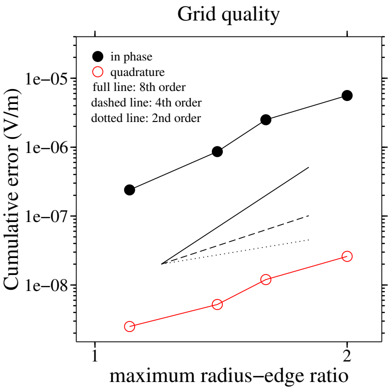

Example 2: accuracy studies

- **Refinement at the line source**
- Line source divided into equal segments

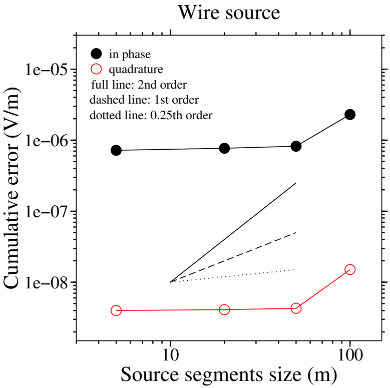

Conclusions

- A finite-volume technique is used for modelling the total field EM data. This technique uses the staggered tetrahedral-Voronoï grid.
- The aim is making use of the features of unstructured grids for efficient modeling of the subsurface and for local refinements in the grid.
- The Helmholtz equation is discretized and solved using a sparse direct solver (MUMPS).
- The scheme has been tested for two models: one with a long grounded wire source; another one for magnetic source-receiver pairs with large conductivity contrasts.
- For the both examples, the results from the FV scheme are in good agreement with those from the literature.
- Accuracy studies show the relatively higher importance of refinement at the observation points and improvement in grid quality, and relatively lower importance of refinement at the sources.

Acknowledgements

- ACOA
  (Atlantic Canada Opportunities Agency)
- NSERC
  (Natural Sciences and Engineering Research Council of Canada)
- Vale

Atlantic Canada Opportunities Agency

NSERC CRSNG

VALE

References

- Amestoy, P. R., Guermouche, A., L'Excellent, J. -Y. and Pralet, S., 2006. Hybrid scheduling for the parallel solution of linear systems, Parallel Computing, 32, 136156.
- Ansari, S. M., and C. G. Farquharson, 2013, Three-dimensional modeling of controlled-source electromagnetic response for inductive and galvanic components: Presented at the 5th International Symposium on Three-Dimensional Electromagnetics.
- Farquharson, C. G., and D. W. Oldenburg, 2002, An integral-equation solution to the geophysical electromagnetic forward-modelling problem, in Three-Dimensional Electromagnetics: Proceedings of the Second International Symposium: Elsevier, 319.
- Farquharson, C. G., Duckworth, K. and D. W. Oldenburg, 2006. Comparison of integral equation and physical scale modeling of the electromagnetic responses of models with large conductivity contrasts, Geophysics, 71, G169-G177.
- Si, H., 2004. TetGen, a quality tetrahedral mesh generator and three-dimensional delaunay triangulator, v1.3 (Technical Report No. 9). Weierstrass Institute for Applied Analysis and Stochastics.